Supplemental material: Quantifying fugitive gas emissions from an oil sands tailings pond with open-path FTIR measurements

Yuan You[1,§], Samar G. Moussa[1], Lucas Zhang[2], Long Fu[2], James Beck[3], Ralf M. Staebler[1]

[1] Air Quality Research Division, Environment and Climate Change Canada (ECCC), Toronto, M3H 5T4, Canada
[2]Alberta Environment and Parks, Edmonton, T5J, 5C6, Canada
[3]Suncor Energy Inc., Calgary, T2P 3Y7, Canada
[§]Now at Department of Physics, University of Toronto, Toronto, M5S 1A7, Canada

Correspondence to: Ralf M. Staebler (ralf.staebler@canada.ca)

1. Map of the measurement site

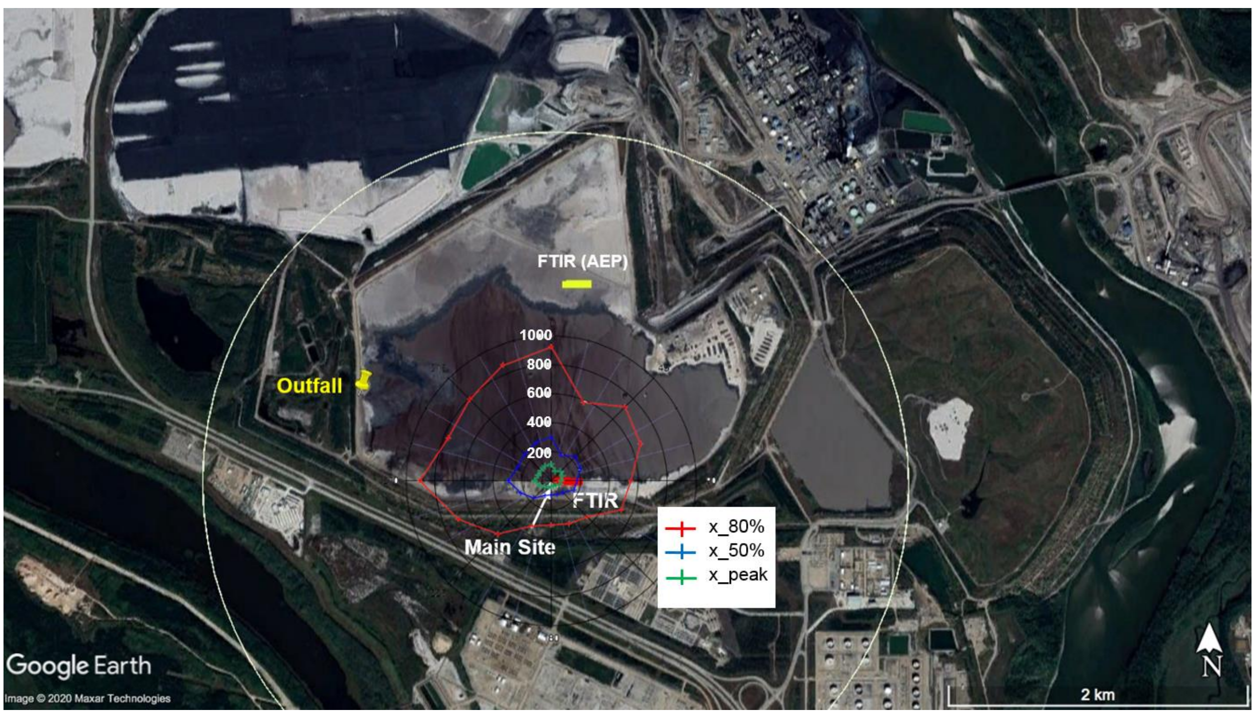

Figure S 1 Map of the site: open-path FTIR on the south shore marked in red, open-path FTIR of AEP on the north shore marked in yellow, and the outfall on the west side. The colored rose plot shows with peak, 50% and 80% contribution distances for eddy covariance fluxes at 18m using the Flux Footprint Prediction (FFP) model (Kljun et al. (2015); You et al. (2020) Fig. S3(b)). The unit of contribution distances is in meters. The white dashed circle labels the 2.3 km distance from the main site, equivalent to 100 times the height of the highest point of the top FTIR path.

2. Methane mole fractions, vertical profiles, and gradient fluxes

2.1 Calibration of retrieved CH_4 mole fraction from OP-FTIR

The amplitude of spectra for all the three paths varied substantially over the study period, especially for the top path. As a proxy for the spectral amplitude, the signal-to-noise ratio (SNR) of the CH_4 fitting was used. The CH_4, NH_3, CH_3OH and HCHO mole fraction for all three paths when this SNR dropped fast, or stayed below 10 were flagged. 3% and 13% of the measurements from bottom and top path were flagged and invalidated from further mole fraction gradient and flux calculations.

Since CH_4 mole fraction was also continuously measured by cavity ring-down spectroscopy (CRDS) at four heights during the study, the measurements at 4m were compared to CH_4 mole fraction retrieved from the FTIR bottom path to calibrate the retrieved CH_4 mole fraction from three paths of this OP-FTIR system.

Each CRDS in this study was calibrated before and after the campaign, and CH_4 mole fraction from three CRDS at the same height was well compared (r^2>0.96, slope=0.98- 1.01, intercept=0.01-0.02 ppm). Therefore, CH_4 mole fraction retrieved from FTIR all three paths were calibrated by the linear relationship in Fig. S2:

$$[CH_4]\_FTIR\_calibrated=1.211\times[CH_4]\_FTIR\_retrieved - 0.379 \qquad (S. 1)$$

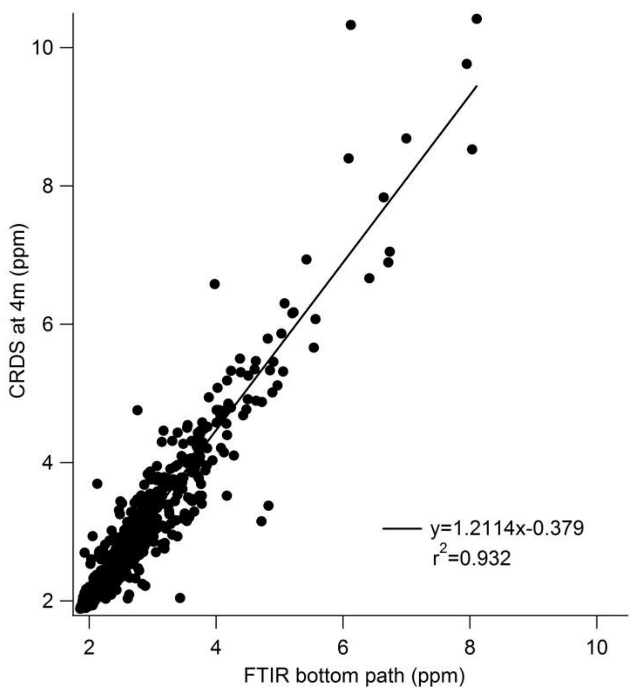

Figure S 2 CH_4 mole fraction retrieved from FTIR bottom path compared to CH_4 mole fraction measured by CRDS (G2204) at 4m. Data are half-hour averaged results.

2.2 Mole fractions and vertical profiles with gradient fluxes

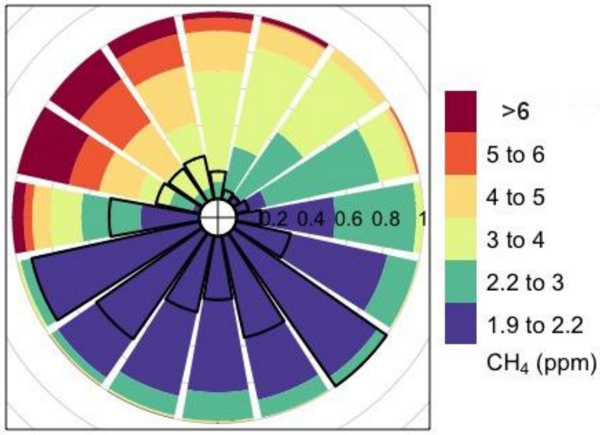

Figure S 3 Normalised rose plot of CH_4 mole fractions from FTIR bottom path. Colors represent CH_4 mole fractions. The length of each colored segment presents the time fractions of that mixing ratio in each direction bin. The radius of the black open sectors indicates the frequency of wind in each direction bin; angle represents wind direction.

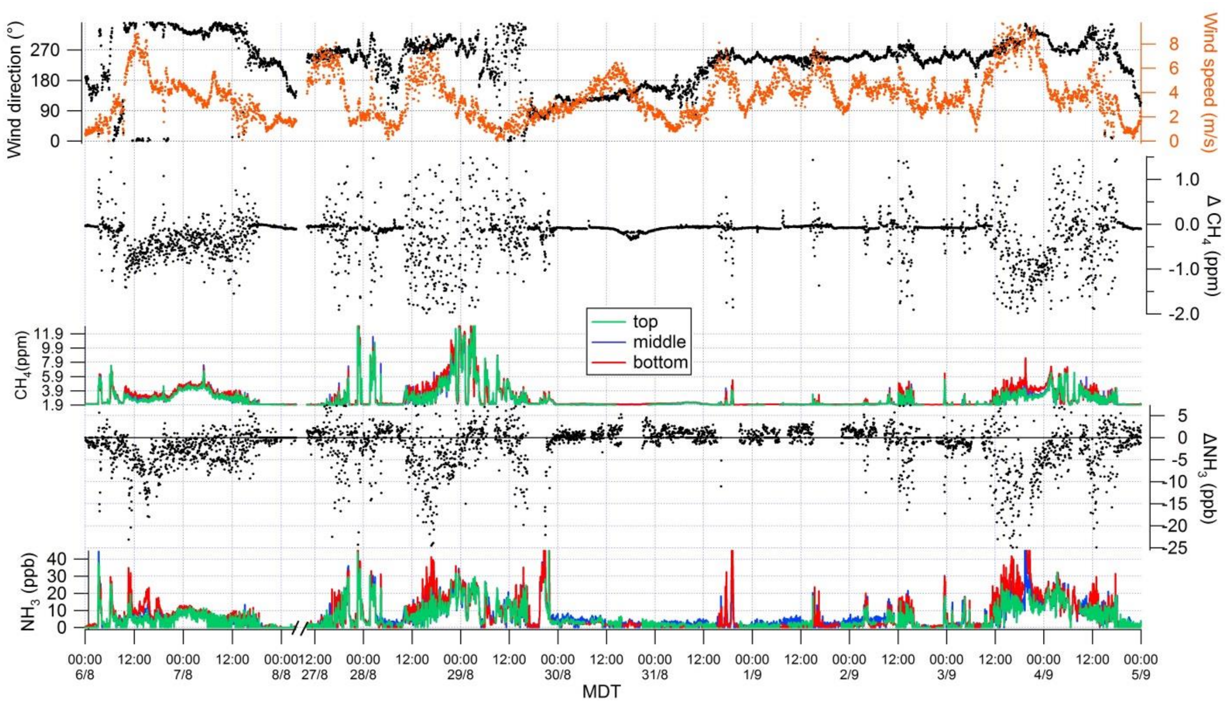

Figure S 4 Time series of wind direction, wind speed, difference in CH_4 mole fractions from the top and bottom paths, CH_4 mole fractions, difference in NH_3 mole fractions from the top and bottom paths, and NH_3 mole fractions, from Aug 6th to 8th, and from Aug 27th to Sept 5th. MDT = Mountain Daylight savings Time.

In the analysis of methane vertical profile below, all the mole fractions measurements (half-hour averages) were taken from the Picarro G2204 at 4, 8, 18, and 32m. There are 271 half-hours in total when the wind was from the pond. About 83% of the half-hour periods when the wind was from the pond direction, the CH_4 vertical profiles are similar to Fig. S4. Within this 83% of periods, some profiles are close to linear, and others are not strict decreasing trend with height. For the rest of 17% of half-hour periods, the CH_4 vertical profiles are closer to logarithmic (Fig. S6). Therefore, CH_4 vertical profiles are considered linear over the entire period for calculating gradient flux with OP-FTIR measurement.

In addition, those half-hour periods when logarithmic relationship is better than linear to describe the vertical profile are mainly (65%) associated with wind speed greater than 6m/s (Fig. S7). For the majority of the time (85%) when the wind was from the pond, wind speed was less than 6m/s (Fig. S7).

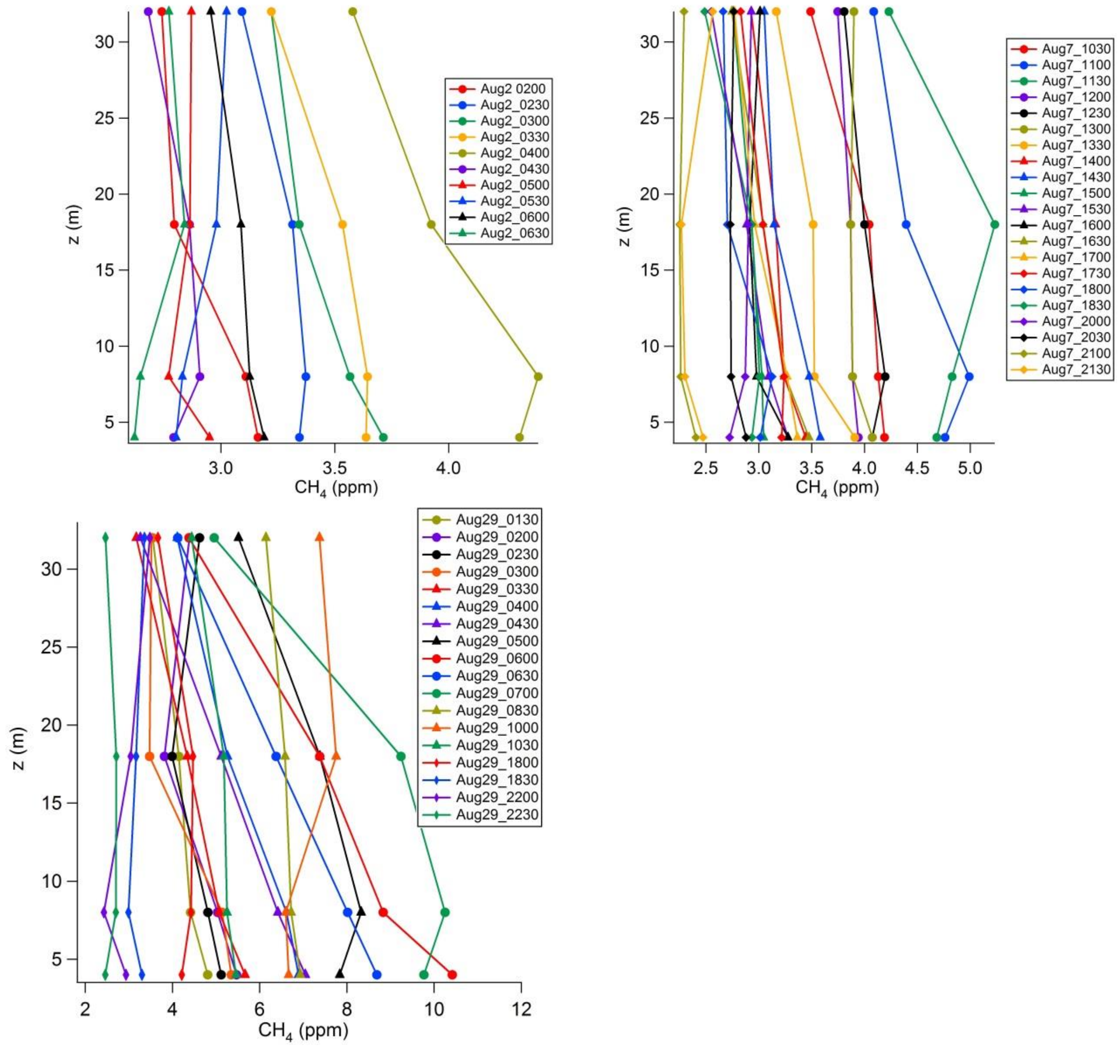

Figure S 5 Examples of observed CH_4 mole fractions vertical profile, when the profiles are close to linear.

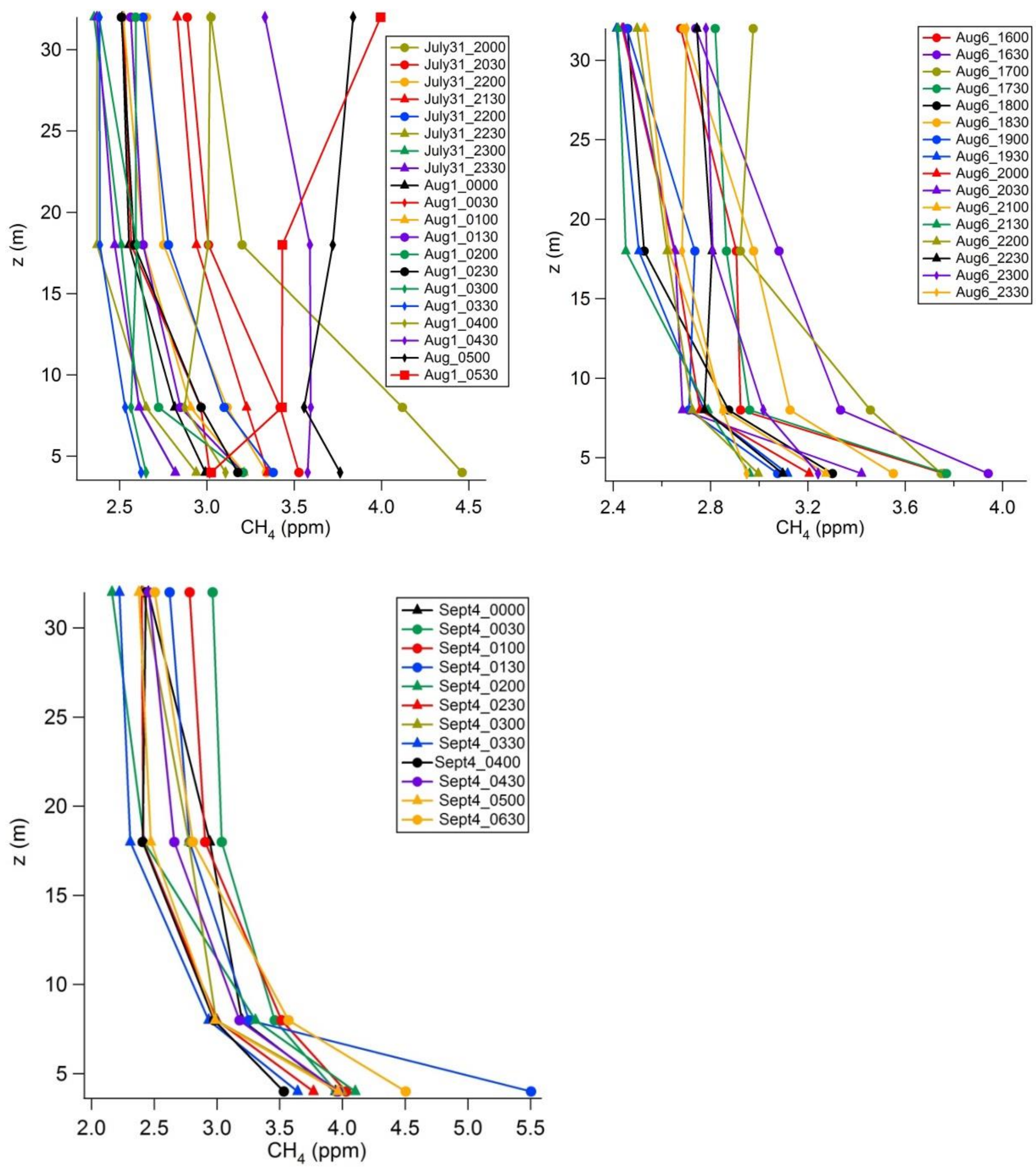

Figure S 6 Examples of observed CH_4 mole fractions vertical profile, when the profiles are close to logarithmic.

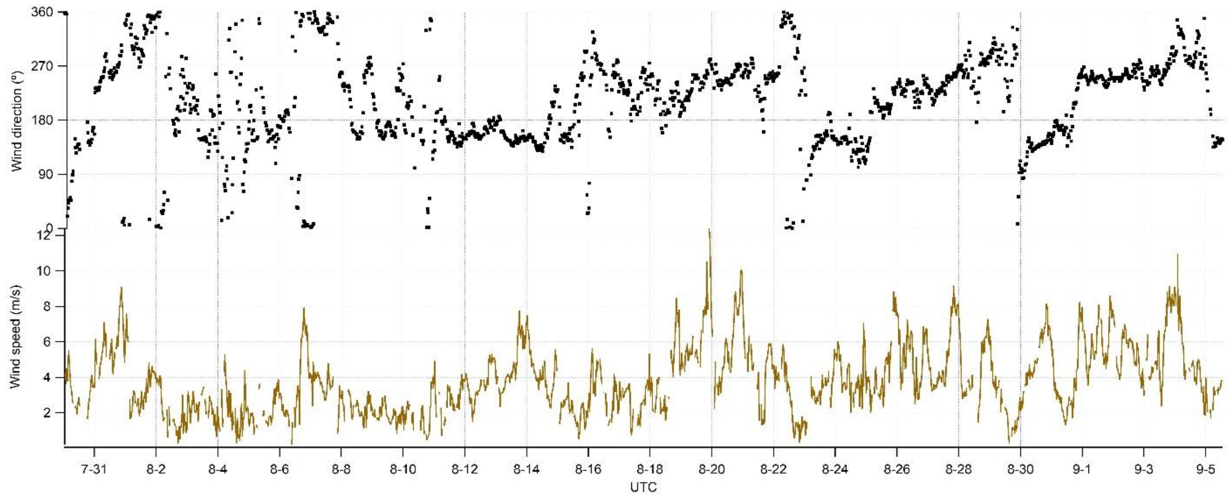

Figure S 7 Time series of wind direction and wind speed measured at 18m over the entire project.

To compare to the assumption of linear vertical profile of CH_4 mole fractions, the calculation of K_c for the assumption of logarithmic vertical profile is also listed here. The representative average height of the FTIR top path with a logarithmic vertical profile would be $Z_{top} = \sqrt{12 \times 1} = 3.5\ m$. Then, K_c for gradient flux calculated from the top-to-bottom path gradient is adjusted logarithmically based on the $K_{c\_2,4}$ calculated from point measurements at 8m and 32m on the tower:

$$\frac{K_{c\_FTIR\_log}}{K_{c\_2,4}} = \frac{\sqrt{3.46\times1}}{\sqrt{8\times32}} = 0.116 \qquad \text{(S. 2)}$$

$$F_{gradient_{FTIR}} = -K_{c\_FTIR\_log} \times \frac{\partial c}{\partial z} = \frac{-K_{c_{FTIR\_log}} * \partial c}{z * \ln(\frac{z_2}{z_1})} = -0.116 \times K_{c_{2,4}} \times \frac{\partial c}{\sqrt{3.46\times1}\times\ln(\frac{3.46}{1})} = -0.0503 \times K_{c_{2,4}} \times \partial c \quad \text{(S.3)}$$

where z is the height for which flux is calculated (Thompson and Pinker, 1981).

If assuming linear vertical profile of CH_4 mole fractions, and plugging in equation (2) in the main text:

$$F_{gradient_{FTIR}} = -K_{c\_FTIR} * \frac{\partial c}{\partial z} = -0.325 * K_{c_{2,4}} * \frac{\partial c}{\frac{12+1}{2} - 1} = -0.0591 * K_{c_{2,4}} * \partial c \quad (S.4)$$

Comparing equations (S.3) and (S.4), the gradient flux calculated with logarithmic vertical profile is 85% of the gradient flux calculated with linear vertical profile.

Beside top-bottom paths of CH_4 mole fractions gradient, middle-bottom paths of gradient can also be used to calculate CH_4 gradient fluxes. The results are summarised in the first row of Table S1 to compare to gradient fluxes with top-bottom paths CH_4 gradients. The area-weighted averaged fluxes with middle-bottom paths is 95% of the area-weighted averaged fluxes with top-bottom paths (Table S1).

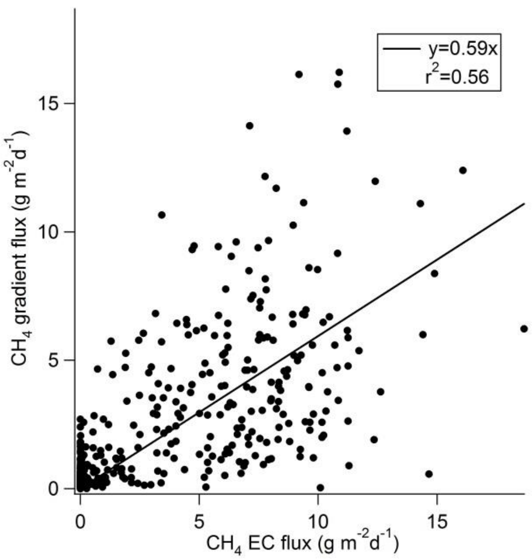

Figure S 8 CH_4 gradient flux from FTIR compared with EC flux.

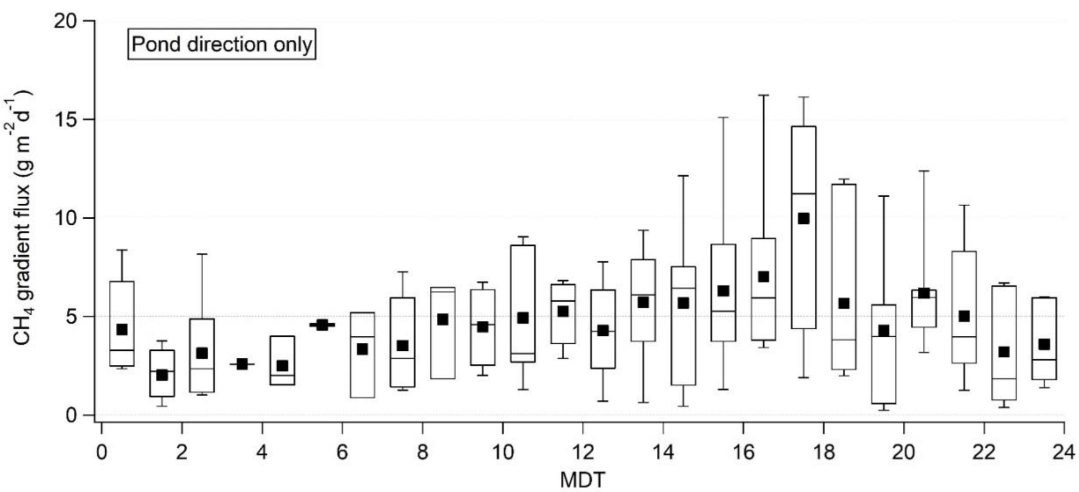

Figure S 9 Diurnal variation of CH_4 gradient flux from FTIR, when the wind came from the pond direction. MDT = Mountain Daylight savings Time.

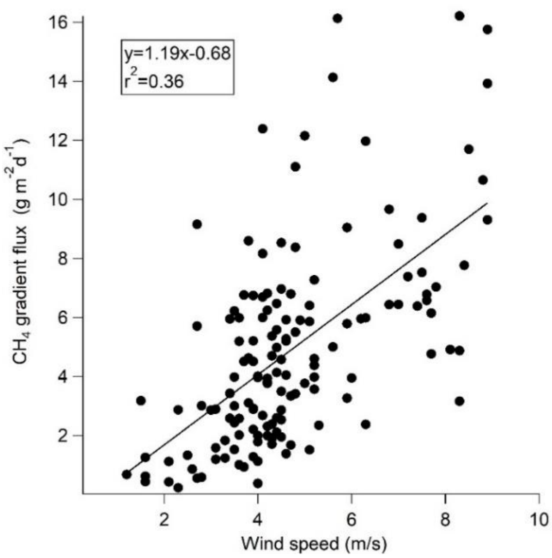

Figure S 10 CH_4 gradient flux when the wind was from the pond.

2.3 IDM flux of CH4 with two approaches of determining background mole fraction input

IDM fluxes of CH_4 with input from FTIR. Fluxes comparison with background mole fraction using ECCC measurement at south, and AEP measurements at north:

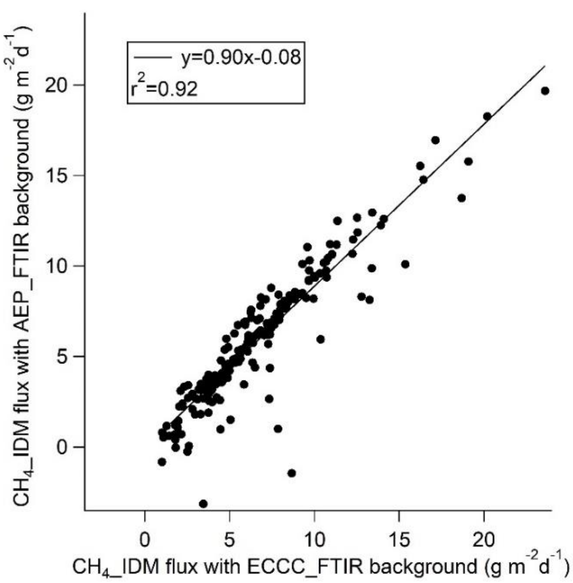

Figure S 11 comparison of CH_4 IDM fluxes with input background mole fraction from the south and north measurements.

The half-hour IDM fluxes with these two approaches agree well (slope = 0.9, r^2=0.92). The sector-area-weight-averaged IDM fluxes with two approaches are also within 20% difference. The interquartile ranges overlap (Table S1).

3. NH_3

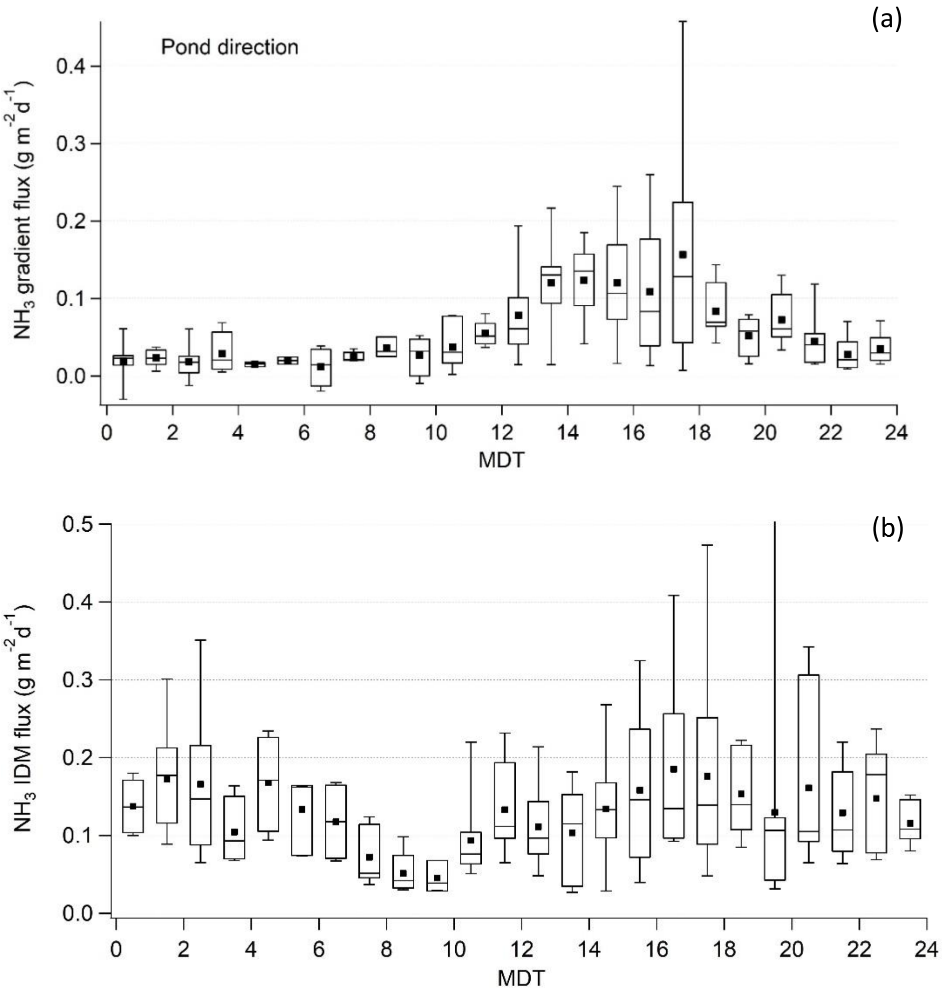

Figure S 12 Diurnal variations of NH_3 gradient flux derived from top-bottom paths (a) and IDM flux (b) when the wind was from the pond direction. MDT = Mountain Daylight savings Time.

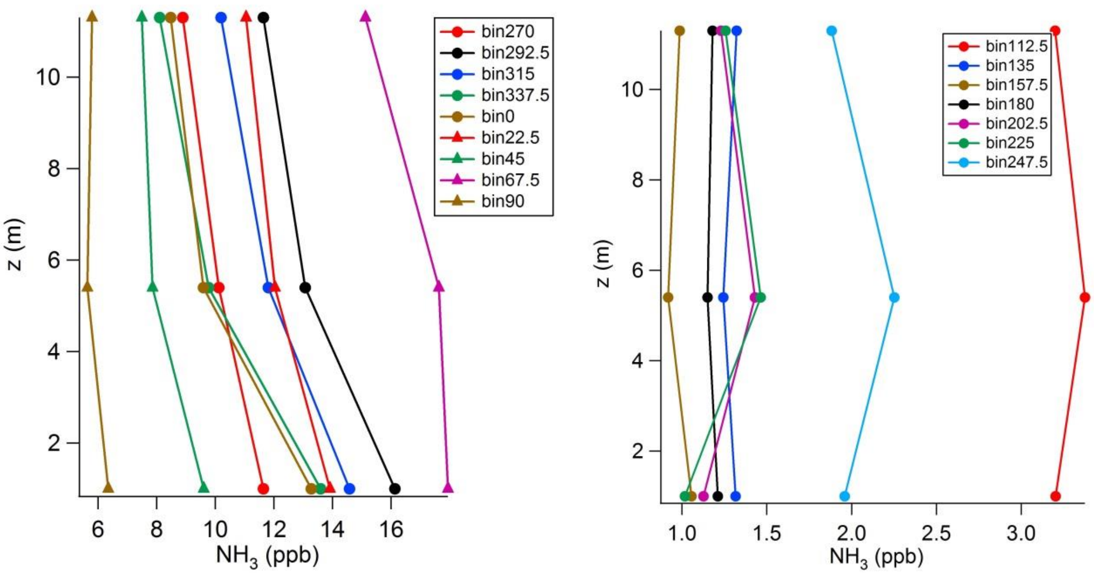

Figure S 13 NH_3 mole fraction vertical profile after averaging in 16 wind direction sectors. The height z for the three paths are the height of the middle point of each path.

4. Total alkane

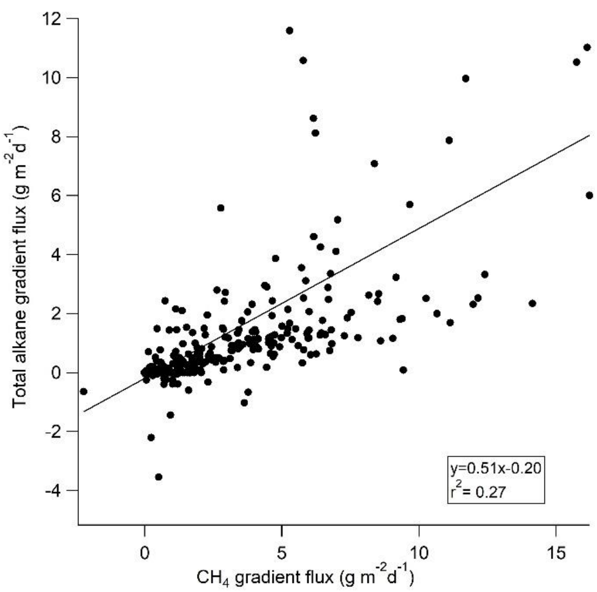

Figure S 14 Total alkane gradient flux compared to CH_4 gradient flux, both derived from OP-FTIR top and bottom paths.

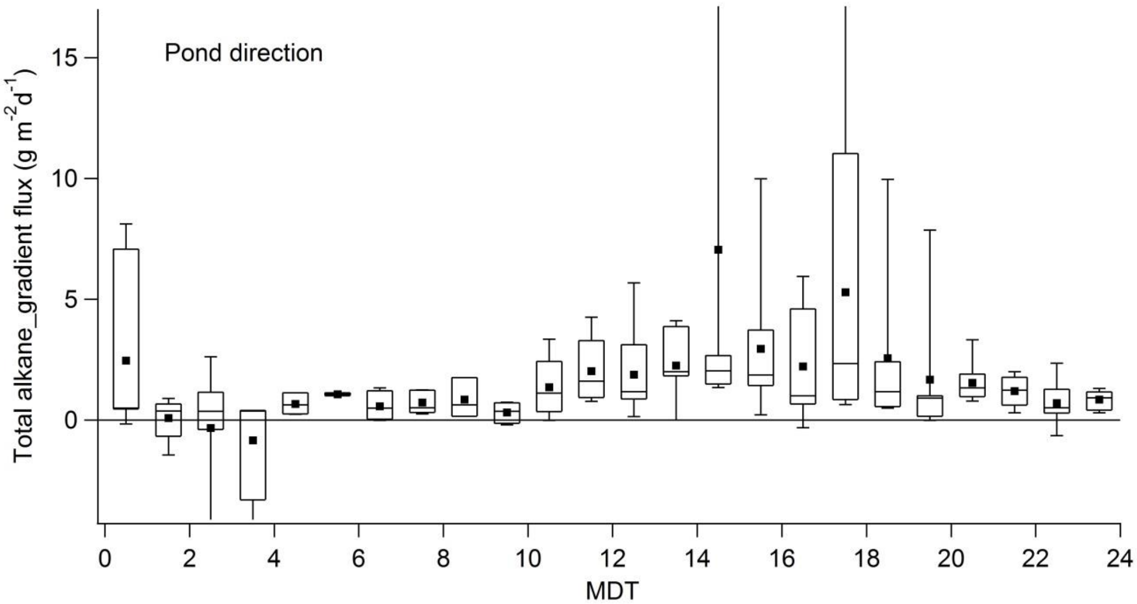

Figure S 15 Diurnal variation of total alkane gradient flux when the wind was from the pond direction. MDT = Mountain Daylight savings Time.

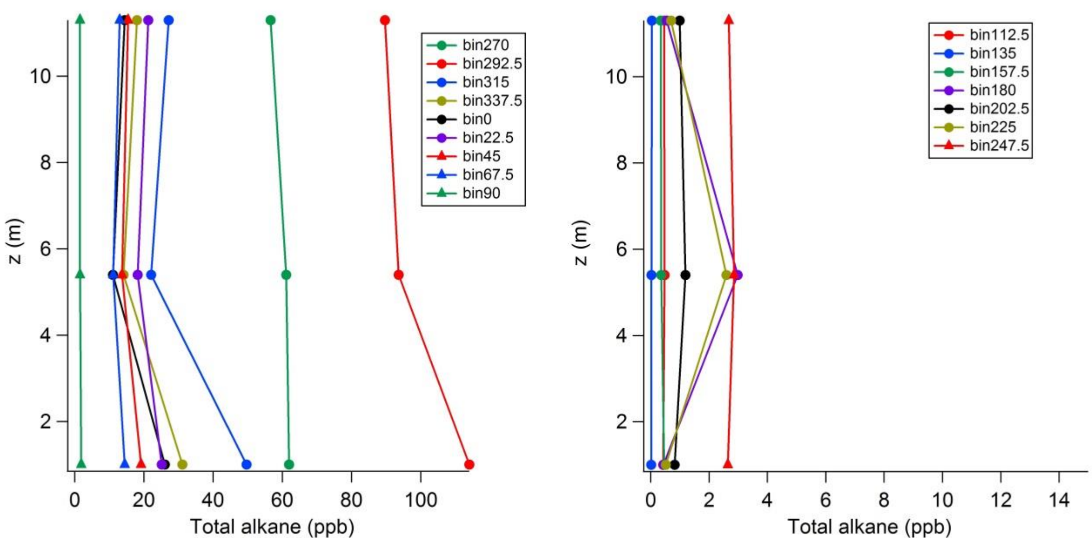

Figure S 16 Total alkane mole fraction vertical profile after averaging in 16 wind direction sectors. The height z for the three paths are the height of the middle point of each path.

5. Methanol (CH_3OH)

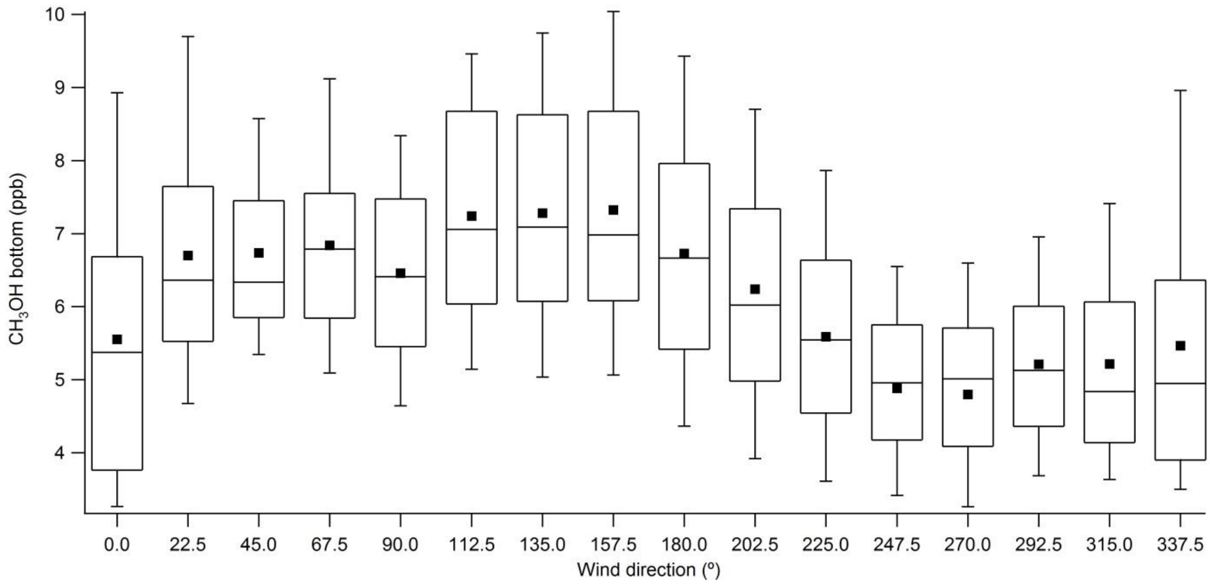

Figure S 17 CH_3OH mole fraction retrieved from the FTIR bottom path, binned in 22.5° sectors.

6. Flux results with the slant path approach from Flesch et al. (2016)

As briefly discussed in the introduction of the main text, Flesch et al., (2016) deployed OP-FTIR measurement with "slant path" configuration, and derived emission rates of N_2O and NH_3 by flux-gradient method. To compare the methods we used to calculate gradient fluxes with their approach, we also performed similar calculation. The derived u_* and L directly from sonic anemometer measurement at 8m on the tower, concentration difference between top and bottom path of FTIR, and calculated S_c were plugged in equation (9) in Flesch et al., (2016). In this study, calculated S_c is allowed to vary with dynamic stability (You et al. (2020) Fig. 3), while in Flesch et al. (2016) S_c was a constant 0.64. The time series of half-hour gradient fluxes of CH_4, NH_3 and total alkane were calculated. Area weight-averaged fluxes were calculated and summarized in Table S1. Compared to gradient flux results with our approach modified Bowen ratio, CH_4, NH_3 and total alkane fluxes with the "slant path" flux-gradient method are 27%, 40%, and 56% smaller.

Tables

Table S1 Summary of CH_4 IDM fluxes with two background approaches, and gradient fluxes with approach from Flesch et al. (2016).

($g\ m^{-2}\ d^{-1}$)	Q_25%	median	Q_75%	mean[a]
CH_4_gradient flux with middle-bottom paths	1.5	3.2	4.9	3.5 ± 1.0
CH_4_IDM flux_with ECCC background	3.6	5.2	6.6	5.4 ± 0.4
CH_4_IDM flux_with AEP background	2.9	4.4	5.6	4.3 ± 0.6
CH_4 gradient flux with approach from Flesch et al. (2016)	1.3	2.2	3.8	2.7 ± 0.9
NH_3 gradient flux with approach from Flesch et al. (2016)	0.01	0.02	0.05	0.03 ± 0.01
Total alkane gradient flux with approach from Flesch et al. (2016)	0.11	0.38	0.88	0.59 ± 0.09

[a] Errors with the mean fluxes are calculated with an integrative approach: the average of observed standard deviations of fluxes from five periods when the fluxes were relatively steady.

Reference

Kljun, N., Calanca, P., Rotach, M. W., and Schmid, H. P.: A simple two-dimensional parameterisation for Flux Footprint Prediction (FFP), Geosci. Model Dev., 8, 3695-3713, http://doi.org/10.5194/gmd-8-3695-2015, 2015.

Thompson, O. E., and Pinker, R. T.: An error analysis of the Thornthwaite-Holzman equations for estimating sensible and latent heat fluxes over crop and forest canopies, J. Appl. Meteorol., 20, 250-254, 1981.